HHS Public Access

Author manuscript

Pancreatology. Author manuscript; available in PMC 2022 March 01.

Published in final edited form as:

Pancreatology. 2021 March ; 21(2): 342–352. doi:10.1016/j.pan.2021.01.007.

Mouse model suggests limited role for human mesotrypsin in pancreatitis

Dóra Mosztbacher[1], **Miklós Sahin-Tóth**[1,2,*]

[1]Center for Exocrine Disorders, Department of Molecular and Cell Biology, Boston University, Henry M. Goldman School of Dental Medicine, Boston, Massachusetts 02118

[2]Department of Surgery, University of California Los Angeles, Los Angeles, California 90095

Abstract

Mesotrypsin is a low-abundance human trypsin isoform with a unique evolutionary mutation that conferred resistance to trypsin inhibitors and restricted substrate specificity. Mesotrypsin degrades the serine protease inhibitor Kazal type 1 (SPINK1) and thereby might increase risk for pancreatitis. Here, we report a mouse model designed to test the role of mesotrypsin in pancreatitis. We introduced the human mesotrypsin evolutionary signature mutation into mouse cationic trypsinogen (isoform T7), resulting in a Gly to Arg change at the corresponding position 199. In biochemical experiments using purified proteins, the p.G199R T7 mutant recapitulated all salient features of human mesotrypsin. *T7G199R* mice developed normally with no spontaneous pancreatitis or other obvious phenotypic changes. Cerulein-induced acute pancreatitis in C57BL/6N and *T7G199R* mice showed similar severity with respect to inflammatory parameters and acinar cell necrosis while plasma amylase activity was higher in *T7G199R* mice. Neither SPINK1 degradation nor elevated intrapancreatic trypsin activation was apparent in *T7G199R* mice. The results indicate that in *T7G199R* mice the newly created mesotrypsin-like activity has no significant impact on cerulein-induced pancreatitis. The observations suggest that human mesotrypsin is unimportant for pancreatitis; a notion that is consistent with published human genetic studies.

Keywords

pancreatitis; trypsin; chymotrypsin; protease activation; SPINK1

[*]Correspondence to Miklós Sahin-Tóth, 675 Charles E Young Drive South, MacDonald Research Laboratories, Rm 2220, Los Angeles, CA 90095. Tel: (310) 267-5905; msahintoth@mednet.ucla.edu.

AUTHOR CONTRIBUTIONS

MST conceived and directed the study. MST and DM designed the experiments. DM performed the experiments. DM and MST analyzed the data. MST wrote the manuscript; DM prepared the figures; both authors contributed to revisions and approved the final version.

CONFLICT OF INTEREST STATEMENT

The authors have declared that no conflict of interest exists.

INTRODUCTION

Inappropriate, early activation of the digestive proenzyme trypsinogen to active trypsin inside the pancreas is a fundamental mechanism of pancreatitis development [1]. In humans, trypsinogen is produced in three isoforms, encoded by separate genes [2]. About 95% of secreted trypsinogen consists of two abundant isoforms, cationic and anionic trypsinogen, the products of the serine protease 1 (PRSS1) and 2 (PRSS2) genes, respectively [3, 4]. The remaining 5% corresponds to mesotrypsinogen (PRSS3), which gives rise to mesotrypsin, a bizarre yet fascinating protease; first identified by Heinrich Rinderknecht in 1978 as an inhibitor-resistant human trypsin [5, 6]. Mesotrypsin is poorly inhibited by polypeptide trypsin inhibitors including the human serine protease inhibitor Kazal type 1 (SPINK1), a 6.2 kDa protein which protects the pancreas against intrapancreatic trypsin activity [5–12]. Remarkably, mesotrypsin recognizes trypsin inhibitors as substrates and cleaves their reactive-site peptide bonds resulting in impaired inhibitory activity [9–14]. In case of human SPINK1, mesotrypsin attacks additional peptide bonds and degrades the inhibitor [9]. Based on this unique property, it was proposed that mesotrypsin evolved specifically for the inactivation and/or degradation of dietary trypsin inhibitors [9]. As a digestive typsin, mesotrypsin exhibits unusually restricted substrate specificity and cleaves most protein substrates poorly. Unlike cationic and anionic trypsin, mesotrypsin cannot activate other protease zymogens, and mesotrypsinogen cannot autoactivate [9, 15]. However, mesotrypsin cleaves Lys/Arg-Ser/Thr peptide bonds relatively well, and it activates proteinase-activated receptors [16–19].

The structural basis of the peculiar characteristics of mesotrypsin lies in an evolutionary mutation that introduced Arg198 (Arg193 in crystallographic numbering) in place of a Gly residue that is strictly conserved in other trypsin isoforms [7–11]. Arg198 occupies the S2’ subsite of the substrate binding site where the extra bulk and the positive charge interfere with inhibitor and substrate binding [8, 10]. Mutation of Arg198 back to Gly restores inhibitor sensitivity and normalizes digestive activity [9]. Mesotrypsin evolved additional residues that facilitate trypsin inhibitor digestion, however, relative to Arg198, their effects are minor [14]. For further details on the biochemical, structural and mechanistic aspects of mesotrypsin, the reader is referred to two published review articles [20, 21].

Human genetic studies established that mutations in PRSS1 increase trypsinogen activation and cause hereditary pancreatitis or sporadic chronic pancreatitis while a mutation in PRSS2, which facilitates degradation, affords some protection against chronic pancreatitis [1]. Recent mouse models confirmed that increased autoactivation of mutant cationic trypsinogen can drive pancreatitis onset and progression [22, 23]. The role of mesotrypsin in pancreatitis has remained hypothetical. The ability of mesotrypsin to degrade protective SPINK1 suggests that it may increase pancreatitis risk or promote its progression. Alternatively, it may modify the disease course through activation of proteinase-activated receptors even in the presence of SPINK1. However, genetic analysis demonstrated no association between chronic pancreatitis and PRSS3 variants and animal models of human mesotrypsin have been lacking [24–27]. Here, we set out to fill this knowledge gap and report the generation and characterization of a novel mouse model designed to study the effect of mesotrypsin-like activity on pancreatitis.

METHODS

Materials.

Protease substrates Z-Gly-Pro-Arg-*p*-nitroanilide (GPR-pNA, catalog number 4000768), Suc-Ala-Ala-Pro-Phe-*p*-nitroanilide (AAPF-pNA, catalog number 4002299), Boc-Gln-Ala-Arg-7-amino-4-methylcoumarin (QAR-AMC, catalog number 4017019), Z-Gly-Pro-Arg-7-amino-4-methylcoumarin (GPR-AMC, catalog number 4002047) and Suc-Ala-Ala-Pro-Phe-7-amino-4-methylcoumarin (AAPF-AMC, catalog number 4012873) were purchased from Bachem USA (Torrance, CA). Free 7-amino-4-methylcoumarin (AMC, catalog number A9891) and cerulein (catalog number C9026) were from MilliporeSigma.

Accession numbers and nomenclature.

NC_000072.6, *Mus musculus* strain C57BL/6J chromosome 6, GRCm38.p6 C57BL/6J; NM_023333.4, *Mus musculus* RIKEN cDNA 2210010C04 gene (2210010C04Rik) mRNA, encoding mouse cationic trypsinogen (isoform T7); NM_009258.5, *Mus musculus* serine peptidase inhibitor, Kazal type 1 mRNA (*Spink1*, legacy name *Spink3*). Amino-acid residues in T7 trypsinogen were numbered from the initiator methionine. Due to an additional amino acid in the activation peptide, numbering in T7 trypsinogen is shifted by one relative to human trypsinogens [28]. The legacy name of the mouse ortholog of human SPINK1 is SPINK3. To avoid confusion, in the present study we use the mouse SPINK1 designation.

Mutagenesis, expression and purification of mouse T7 trypsinogen.

The pTrapT7-intein-mouse-T7 plasmid encoding a fusion between a self-splicing mini-intein and mouse cationic trypsinogen was described previously [22]. Mutation p.G199R was introduced by overlap extension PCR mutagenesis. Wild-type and p.G199R mutant intein-trypsinogen fusions were expressed in *E. coli* LG-3, the inclusion bodies were isolated and subjected to *in vitro* refolding [29]. Trypsinogen was then purified using ecotin affinity-chromatography [29, 30]. Concentration of trypsinogen solutions was calculated from their UV absorbance at 280 nm using the extinction coefficient 39,140 $M^{-1}cm^{-1}$.

Expression and purification of mouse SPINK1 and chymotrypsinogen B1 (CTRB1).

The pcDNA3.1(−) expression plasmid for mouse CTRB1 with a C-terminal 10His tag was described previously [31]. The coding region of mouse SPINK1 (legacy name SPINK3) with a C-terminal 10His tag was custom-synthesized and cloned into the pcDNA3.1(−) plasmid using the restriction sites XhoI and BamHI. To boost expression, His-tagged mouse SPINK1 was subsequently engineered into a previously described minigene containing intron 1 of human SPINK1 [32]. In this construct, the intron is placed in the appropriate context between exon 1 and exons 2–4 of SPINK1. Mouse CTRB1 and SPINK1 were then expressed in transiently transfected HEK 293T cells and purified using nickel-affinity chromatography, as reported earlier [33]. The peak fractions eluted from the nickel column were pooled and dialyzed against 0.1 M Tris–HCl (pH 8.0), 150 mM NaCl. CTRB1 concentration was estimated form the UV absorbance at 280 nm using the extinction

coefficient 53,105 $M^{-1}cm^{-1}$. The concentration of SPINK1 was measured by titration against T7 trypsin.

Trypsinogen autoactivation.

Trypsinogens at 2 μM concentration were incubated with 10 nM initial trypsin in 0.1 M Tris-HCl (pH 8.0), 1 mM $CaCl_2$, and 0.05% Tween 20 (final concentrations), in 200 μL final volume, at 37°C. Aliquots (1.5 μL) were removed at the indicated time points and mixed with 48.5 μL assay buffer (0.1 M Tris-HCl (pH 8.0), 1 mM $CaCl_2$ and 0.05% Tween 20) followed by addition of 150 μL of 200 μM GPR-pNA trypsin substrate, dissolved in assay buffer. Substrate hydrolysis was followed in a microplate reader at 405 nm for 1 min and reaction rates were determined from the linear portion of the curves. Trypsin activity was expressed as percent of the possible maximal activity measured by activation with enteropeptidase.

Kinetic analysis of trypsin activity.

Michaelis-Menten parameters of trypsin activity were measured at 23°C in 0.1 M Tris-HCl (pH 8.0), 1 mM $CaCl_2$, and 0.05% Tween 20 in 200 μL final volume. Trypsinogen was activated with enteropeptidase and 0.5 nM or 1 nM active trypsin (absorbance-based concentration assuming full activation) was used in the assays. The concentration of the indicated peptide substrates was varied between 1.5 and 200 μM. The rates obtained in relative fluorescent units (RFU) per second with the AMC substrates were converted to nM/sec units using an AMC calibration curve. The rates measured in mOD/min units with the pNA substrate were converted to nM/sec units using the extinction coefficient 10,400 M^{-1} cm^{-1}, corrected for the shorter light path of the plate reader (6,770 M^{-1}). Initial rates of substrate cleavage were plotted as a function of substrate concentration and data points were fitted with the Michaelis-Menten hyperbolic equation.

Activation of chymotrypsinogen by trypsin.

Mouse CTRB1 zymogen (1 μM) was incubated with 5 nM wild-type or p.G199R mutant T7 trypsin in 0.1 M Tris-HCl (pH 8.0), 1 mM $CaCl_2$, 0.05% Tween 20 and 2 mg/mL bovine serum albumin (final concentrations) at 37°C. At the indicated times, aliquots (1.5 μL) were removed and mixed with 48.5 μL assay buffer and 150 μL of 200 μM AAPF-pNA chymotrypsin substrate, dissolved in assay buffer. The cleavage reaction was monitored in a microplate reader at 405 nm for 1 min; initial rates were determined and expressed in mOD/min units.

Trypsin inhibition by mouse SPINK1.

Wild-type and p.G199R mutant T7 trypsin (5 nM final concentration) were incubated with the indicated concentrations of SPINK1 in assay buffer, at 23 °C, for 60 min, in 200 μL final volume. The residual trypsin activity was then measured by adding 5 μL of 6 mM GPR-pNA substrate.

Digestion of SPINK1 and casein by trypsin.

Mouse SPINK1 at 2.1 μM concentration was incubated with 100 nM wild-type or G199R mutant T7 trypsin in 0.1 M Tris-HCl (pH 8.0) and 1 mM $CaCl_2$ (final concentrations) at 37°C. Bovine β-casein (catalog number C6905, MilliporeSigma) was incubated at 0.2 mg/mL concentration with 5 nM wild-type or p.G199R mutant T7 trypsin in 0.1 M Tris-HCl (pH 8.0) and 1 mM $CaCl_2$ (final concentrations) at 37°C. Aliquots (100 μL) were withdrawn at the indicated time points and the proteins were precipitated by adding 15 μL 100% trichloroacetic acid solution. Precipitates were collected by centrifugation and dissolved in 17.7 μL 2x Laemmli sample buffer (catalog number 161–0737, Bio-Rad, Hercules, CA) plus 1.8 μL 1M dithiothreitol and 0.5 μL 5N NaOH. The samples were then denaturated at 95°C for 5 min, electrophoresed on 15% SDS-polyacrylamide minigels and stained with Brilliant Blue R-250. PageRuler Prestained Protein Ladder, 10 to 180 kDa (catalog number 26617, Thermo Scientific) was used as molecular weight markers.

Animal studies protocol approval.

All mouse experiments were performed at Boston University with the approval and oversight of the Institutional Animal Care and Use Committee (IACUC), including protocol review and post-approval monitoring. The animal care program at Boston University is managed in full compliance with the US Animal Welfare Act, the United States Department of Agriculture Animal Welfare Regulations, the US Public Health Service Policy on Humane Care and Use of Laboratory Animals and the National Research Council's Guide for the Care and Use of Laboratory Animals. Boston University has an approved Animal Welfare Assurance statement (A3316–01) on file with the US Public Health Service, National Institutes of Health, Office of Laboratory Animal Welfare and it is accredited by the Association for Assessment and Accreditation of Laboratory Animal Care International (AAALAC).

Generation of the *T7G199R* mouse strain.

The gene encoding T7 trypsinogen (2210010C04Rik) is located on chromosome 6; it spans ~3.8 kb and comprises 5 exons. Mutation c.595G>C (p.G199R) was introduced by homologous recombination in C57BL/6 embryonic stem (ES) cells (Cyagen, Santa Clara, CA). The targeting vector contained the T7 trypsinogen gene with the p.G199R mutation in exon 5 and the neomycin resistance gene flanked by loxP sites in intron 4 (Supplementary Figure 1). Correctly targeted ES cell clones were identified by long-range PCR and verified by Southern blot. Mutant ES cells were injected into mouse embryos (blastocysts), which were implanted into pseudopregnant females. The resulting chimeras were bred with a Cre-deleter strain to achieve germline transmission of the mutant allele and to remove the neomycin resistance gene. The final *T7G199R* allele contained the p.G199R mutation in exon 5 and a 120 nt residual sequence in intron 4 including a single loxP site (Supplementary Figure 2). *T7G199R* mice were maintained in the homozygous state. C57BL/6N mice purchased from Charles River Laboratories (Wilmington, MA) or produced in our breeding facility from the same stock were used as experimental controls. The number of animals used in each experiment is shown in the figures. Both male (51%) and female

(49%) animals were studied. Experimental mice were 8–11 weeks old and weighed 23.4±2.1 g (males, mean±SD) and 18.1±1.7 g (females, mean±SD).

Genotyping.

To genotype the *T7G199R* strain, we designed PCR primers to amplify exon 5 and the flanking sequences of the T7 trypsinogen gene (Supplementary Figure 2). The wild-type amplicon was 517 bp, while the mutant allele yielded a product of 637 bp, because of the residual sequence in intron 4. The primer sequences were as follows. Forward: 5’ - CAA ACA TTT TAT CTG ACC GTG TAC C - 3’; Reverse: 5’ - TGG ATT TGA CAA CAA AGA GAG GGC - 3’.

Quantitative reverse-transcription PCR.

RNA from ~30 mg pancreas tissue was isolated and reverse-transcribed as described previously [31]. Levels of T7 trypsinogen mRNA were determined as reported earlier [23] with the exception that the reference gene was *Rpl13a*, measured with the TaqMan Gene Expression Assay Mm01612987_g1 (Life Technologies). Relative expression levels were estimated with the comparative cycle threshold method (ΔΔCt method).

Western blotting.

Pancreas tissue (30–40 mg) was homogenized in 300–400 μL phosphate-buffered saline (pH 7.4) containing 3–4 μL Halt Protease and Phosphatase Inhibitor Cocktail (catalog number 78440, ThermoFisher Scientific). The homogenate was centrifuged (10 min, 13,500 rpm, 4°C) and the supernatant (30 μg total protein per well) was electrophoresed on 15% mini-gels together with PageRuler Prestained Protein Ladder, 10 to 180 kDa (catalog number 26617, Thermo Scientific) molecular weight markers. After transfer to PVDF membrane, western blotting was performed with the following antibodies. A custom-made rabbit polyclonal antibody against T7 trypsinogen was used at 1:10,000 dilution [22]; a rabbit polyclonal antibody against mouse SPINK1 (catalog number 2744S, SPINK3 antibody, Cell Signaling Technology, Danvers, MA) was used at 1:500 dilution; and a rabbit monoclonal antibody against mouse ERK1/2 (catalog number 4695, Cell Signaling Technology) was used at 1:500 dilution. HRP-conjugated goat anti-rabbit polyclonal IgG (catalog number 31460, ThermoFisher Scientific) was used as secondary antibody at 1:10,000 dilution after the T7 trypsinogen primary antibody and at 1:20,000 dilution after the mouse SPINK1 and ERK1/2 primary antibodies.

Cerulein-induced acute pancreatitis in mice.

Pancreatitis was induced by repeated intraperitoneal injections of cerulein (50 μg/kg body weight). Cerulein was dissolved in normal saline (10 μg/mL), filter-sterilized and administered 10 times hourly. Injections of normal saline were given to control mice. Mice were sacrificed 1 h after the last injection and the pancreas and blood were harvested. The protocols for pancreas histology and the measurement of plasma amylase activity, pancreas water content, and pancreas myeloperoxidase (MPO) levels were published previously [23, 31].

Intrapancreatic trypsin and chymotrypsin activation.

Cerulein-induced activation of intrapancreatic trypsin and chymotrypsin was measured 30 min after a single injection of cerulein, according to our published method [34]. Control mice were given normal saline injections.

Statistical analysis.

Results were graphed as individual data points with the mean and standard deviation (SD) indicated. The difference of means between two groups was analyzed by unpaired t-test. $P < 0.05$ was considered statistically significant.

RESULTS

The effect of mutation p.G199R on mouse cationic trypsinogen and trypsin.

To model mesotrypsin-like activity in the mouse pancreas, we introduced the evolutionary p.G198R human mesotrypsin signature mutation into mouse cationic trypsinogen (isoform T7). In this isoform, the mutation is designated p.G199R. To demonstrate feasibility of the project, first we compared properties of purified wild-type and p.G199R mutant T7 trypsinogen and trypsin. Remarkably, mutant p.G199R exhibited all known biochemical characteristics of human mesotrypsin (Figures 1, 2). Thus, p.G199R trypsin was resistant to inhibition by mouse SPINK1, while wild-type T7 was fully inhibited (Figure 1A). T7 p.G199R trypsin, but not wild-type T7 trypsin, rapidly cleaved the Arg42-Ile43 reactive-site peptide bond of mouse SPINK1 (Figure 1B). Furthermore, p.G199R trypsinogen lost its ability to autoactivate (Figure 2A) and p.G199R trypsin activated mouse chymotrypsinogen B1 (CTRB1) poorly (Figure 2B). Similarly, p.G199R trypsin did not digest bovine ß-casein, under conditions where wild-type T7 trypsin degraded this protein substrate (Figure 2C). Finally, the p.G199R mutant trypsin readily cleaved small peptide substrates but with altered kinetic parameters relative to wild-type T7 trypsin (Table 1).

Generation of the *T7G199R* mouse strain.

We engineered the p.G199R mutation into exon 5 of the mouse cationic trypsinogen (isoform T7) gene, as described in Methods (Figure 3A). The resultant *T7G199R* mice were bred to homozygosity and maintained in this state. Homozygous *T7G199R* mice developed and bred normally and showed no obvious phenotypic or behavioral changes. Pancreas morphology and histology was also unchanged. We compared T7 trypsinogen expression in the pancreas of C57BL/6N and *T7G199R* mice by quantitative reverse-transcription PCR and western blotting. We found that T7 trypsinogen expression was comparable in the two strains both at the mRNA (Figure 3B) and protein levels (Figure 3C).

Cerulein-induced pancreatitis in *T7G199R* mice.

To evaluate the impact of the mesotrypsin-like activity in *T7G199R* mice on pancreatitis development and severity, we compared pancreatitis responses in *T7G199R* and C57BL/6N mice after 10 hourly injections of supramaximal stimulatory doses of cerulein (Figures 4 and 5). Mice were sacrificed 1 h after the last injection. We measured the cerulein-induced elevations in pancreas mass (Figure 4A,B), pancreatic water content (Figure 4C), plasma

amylase activity (Figure 5A), and MPO content in the pancreas (Figure 5B). When compared to mice given saline injections, all investigated parameters increased significantly in mice given cerulein. We found no significant differences between *T7G199R* and C57BL/6N mice with respect to pancreas mass, water content and MPO levels. When normalized to body mass, the pancreas mass of cerulein-treated *T7G199R* mice was slightly smaller than those of C57BL/6N mice. This seemed biologically insignificant. Interestingly, however, plasma amylase activity was significantly higher in cerulein-treated *T7G199R* mice than in C67BL/6N mice and this effect was seen mostly in male mice, for reasons that are not readily apparent. Evaluation of pancreas sections by hematoxylin-eosin staining revealed no appreciable differences between cerulein-treated *T7G199R* and C57BL/6N mice (Figure 6A). Histology scoring of a large number of pancreas sections (n=17–18) for the characteristic edema (Figure 6B), inflammatory cell infiltration (Figure 6C) and acinar cell necrosis (Figure 6D) confirmed the similar disease severity in *T7G199R* and C57BL/6N mice. Note that the histological edema score was statistically higher in C57BL/6N versus *T7G199R* mice (Figure 6B), however, the difference was biologically unimportant (cf Figure 4C).

SPINK1 expression in cerulein-induced pancreatitis of *T7G199R* mice.

We measured pancreatic SPINK1 levels in *T7G199R* and C57BL/6N mice given 10 hourly injections of cerulein or saline. In the first experiment, we compared the effects of saline versus cerulein treatment on SPINK1 expression. As reported previously [35], we found that SPINK1 was upregulated in cerulein-treated C57BL6/N mice about 2-fold relative to saline-treated controls and a similar but slightly smaller (1.6-fold) increase was evident in *T7G199R* mice (Figure 7A). Next, in a separate experiment, we compared SPINK1 levels in the pancreas of *T7G199R* and C57BL/6N mice given saline or cerulein. No significant differences were observed in the SPINK1 expression of the two strains after either treatment (Figure 7B). Taken together, the observations indicate that during cerulein-induced pancreatitis SPINK1 is upregulated similarly in *T7G199R* and C57BL/6N mice, and significant SPINK1 degradation does not occur in *T7G199R* mice. Cleavage of the reactive-site peptide bond of SPINK1, which would result in a doublet as seen in Figure 1B, was not observed either.

Intrapancreatic protease activation in *T7G199R* mice.

Cerulein-induced intrapancreatic trypsin and chymotrypsin activation was analyzed 30 min after a single cerulein injection. Since the p.G199R mutant trypsin cleaves small peptide substrates differently than wild-type T7 trypsin (see Table 1), we tested intrapancreatic trypsin activation using two different substrates. When measured with the GPR-AMC substrate, the cerulein-induced increase in intrapancreatic trypsin activity was about 40% smaller in *T7G199R* mice relative to C57BL/6N mice (Figure 8A). When the QAR-AMC substrate was used, however, essentially identical increases in trypsin activity were seen in the two strains (Figure 8B). Using the kinetic parameters shown in Table 1, we calculated the substrate cleavage rates at the 150 μM substrate concentration employed in the reactions. Wild-type T7 trypsin cleaved the GPR-AMC substrate 2.5-fold better than the p.G199R mutant, whereas the QAR-AMC substrate was cleaved 1.3-fold better by the mutant trypsin. Thus, the different enzymatic properties of wild-type and p.G199R mutant T7 trypsin

account for the apparent discrepancy between the results of the two experiments and support the conclusion that cerulein-induced intrapancreatic trypsin activation is roughly comparable in *T7G199R* and C57BL/6N mice. The observations are also consistent with the notion that the majority of the trypsin activity originates from the activation of T7 trypsinogen, and the contribution of other trypsinogen isoforms is less important [36, 37]. Finally, cerulein-induced intrapancreatic chymotrypsin activation was about 50% lower in *T7G199R* mice relative to C57BL/6N mice (Figure 8C). This result is readily explained by the impaired ability of the p.G199R mutant T7 trypsin to activate chymotrypsinogen B1 (see Figure 2B).

DISCUSSION

In the present study, we created a novel mouse model to study the role of human mesotrypsin in pancreatitis. To this end, we introduced the human mesotrypsin evolutionary signature mutation into the mouse cationic trypsinogen locus (isoform T7). Biochemical studies confirmed that the p.G199R mutant T7 trypsin has all the characteristic properties of human mesotrypsin: it is resistant to the SPINK1 trypsin inhibitor, it rapidly cleaves the reactive-site peptide bond of SPINK1, it activates chymotrypsinogen poorly and digests casein inefficiently. Unlike wild-type T7 trypsinogen, the p.G199R mutant cannot autoactivate. The pleiotropic effect of the p.G199R mutation on trypsin function may affect pancreatitis by various mechanisms. Hypothetical scenarios predict that (1) inactivation of SPINK1 may render pancreatitis more severe; (2) the inability to autoactivate may reduce intrapancreatic trypsin activation and thereby protect against pancreatitis; (3) inhibitor resistance may increase intrapancreatic trypsin activity and pancreatitis severity. However, these effects may also synergize or antagonize each other resulting in unpredictable pancreatitis phenotypes. Conversion of the native T7 trypsinogen gene to the mesotrypsin-like p.G199R mutant introduced another confounding factor; i.e. the elimination of wild-type T7. However, previous studies demonstrated that genetic deletion of T7 trypsinogen has a relatively small impact on cerulein-induced pancreatitis [36, 37].

We found that severity of cerulein-induced pancreatitis in *T7G199R* and C57BL/6N mice was similar with the sole exception of plasma amylase activity. No difference was seen with respect to inflammation (edema, MPO, inflammatory cell infiltrates) or acinar cell necrosis. Curiously, cerulein treatment caused significantly larger elevations of plasma amylase activity in male *T7G199R* mice relative to C57BL/6N mice. Since other parameters of pancreatitis severity were comparable between the two strains; we cannot offer a simple explanation for this observation. It was proposed previously that during pancreatitis trypsin exerts a secretagogue effect through the activation of proteinase-activated receptors [38]. It is conceivable, even likely, that the p.G199R mutant trypsin activates these receptors differently than wild-type T7 trypsin and this influences pathological amylase release. The apparent gender difference in the plasma amylase activity remains unexplained but it may be related to the different body and pancreas mass of male and female mice used in the experiments.

Levels of protective SPINK1 protein were comparable in the resting (saline-treated) pancreas of *T7G199R* and C57BL/6N mice. Furthermore, during cerulein-induced pancreatitis, intrapancreatic SPINK1 levels increased similarly in the two strains, as reported

previously [35]. We found no evidence of SPINK1 degradation or even cleavage of the reactive-site peptide bond in *T7G199R* mice. These findings were surprising and seem to suggest that during pancreatitis mesotrypsin might not interact with SPINK1 in a manner that modifies SPINK1 levels or activity. We note, however, that in the cerulein-induced pancreatitis model the extent of intrapancreatic trypsin activation is low (relative to the trypsinogen content) and degradation of the small amount of SPINK1 co-localized with active T7 p.G199R trypsin might not be detectable by western blotting.

Cerulein-induced intrapancreatic activation of trypsin was essentially unchanged in *T7G199R* mice relative to C57BL/6N mice. Since the p.G199R T7 trypsinogen mutant cannot autoactivate, the results suggest that cathepsin B-mediated activation is responsible for the observed trypsin activity. Although not shown, biochemical experiments confirmed that the p.G199R T7 mutant is readily activated by cathepsin B. In contrast to trypsin, cerulein-induced intrapancreatic activation of chymotrypsin was reduced in *T7G199R* mice. The p.G199R mutant T7 trypsin activates chymotrypsinogen poorly (see Figure 2B), therefore, the decreased intrapancreatic chymotrypsin activation was predictable.

This novel mouse model should be useful for studying the role of mesotrypsin activity in pancreas physiology and pathology. In this regard, it is noteworthy that mesotrypsin has been implicated in various cancers including pancreatic adenocarcinoma [39–42]. Limitations of the model are related to the conversion of the highly expressed T7 trypsinogen isoform to a mesotrypsinogen-like mutant. Thus, levels of the T7 p.G199R mutant in mice far exceed those of human mesotrypsinogen, which corresponds to less than 5% of total trypsinogens [6]. Furthermore, loss of wild-type T7 trypsinogen in *T7G199R* mice might confound interpretation of the experiments.

Taken the results together and considering all limitations of the model, the most straightforward interpretation of the observations is that the mesotrypsin-like activity in *T7G199R* mice has no significant impact on the severity of cerulein-induced pancreatitis. The implication of these findings is that human mesotrypsin may play no important role in pancreatitis pathogenesis. This notion is in agreement with the absence of association between genetic variants of mesotrypsin (PRSS3) and chronic pancreatitis [24–27]. A recent biochemical study showing that human mesotrypsin is inactivated by chymotrypsin C also implies that mesotrypsin-mediated SPINK1 degradation is unlikely to contribute to the pathogenesis of human pancreatitis [43].

Supplementary Material

Refer to Web version on PubMed Central for supplementary material.

ACKNOWLEDGMENTS

This work was supported by the National Institutes of Health (NIH) grant R01 DK117809 and R01 DK058088 (to MST). DM was also supported by a fellowship from the Rosztoczy Foundation. The authors gratefully acknowledge Zsanett Jancsó, Andrea Geisz and Alexandra Demcsák for technical assistance and helpful discussions.

REFERENCES

1. Hegyi E, Sahin-Tóth M. Genetic risk in chronic pancreatitis: The trypsin-dependent pathway. Dig Dis Sci 2017, 62:1692–1701 [PubMed: 28536777]
2. Chen JM, Férec C. Genes, cloned cDNAs, and proteins of human trypsinogens and pancreatitis-associated cationic trypsinogen mutations. Pancreas 2000, 21:57–62 [PubMed: 10881933]
3. Scheele G, Bartelt D, Bieger W. Characterization of human exocrine pancreatic proteins by two-dimensional isoelectric focusing/sodium dodecyl sulfate gel electrophoresis. Gastroenterology 1981, 80:461–473 [PubMed: 6969677]
4. Rinderknecht H Activation of pancreatic zymogens. Normal activation, premature intrapancreatic activation, protective mechanisms against inappropriate activation. Dig Dis Sci 1986, 31:314–321 [PubMed: 2936587]
5. Rinderknecht H, Renner IG, Carmack C, Friedman R, Koyama P. A new protease in human pancreatic juice. Clin Res 1978, 26:112A
6. Rinderknecht H, Renner IG, Abramson SB, Carmack C. Mesotrypsin: a new inhibitor-resistant protease from a zymogen in human pancreatic tissue and fluid. Gastroenterology 1984, 86:681–692 [PubMed: 6698368]
7. Nyaruhucha CN, Kito M, Fukuoka SI. Identification and expression of the cDNA-encoding human mesotrypsin(ogen), an isoform of trypsin with inhibitor resistance. J Biol Chem 1997, 272:10573–10578 [PubMed: 9099703]
8. Katona G, Berglund GI, Hajdu J, Gráf L, Szilágyi L. Crystal structure reveals basis for the inhibitor resistance of human brain trypsin. J Mol Biol 2002, 315:1209–1218 [PubMed: 11827488]
9. Szmola R, Kukor Z, Sahin-Tóth M. Human mesotrypsin is a unique digestive protease specialized for the degradation of trypsin inhibitors. J Biol Chem 2003, 278:48580–48589 [PubMed: 14507909]
10. Salameh MA, Soares AS, Hockla A, Radisky ES. Structural basis for accelerated cleavage of bovine pancreatic trypsin inhibitor (BPTI) by human mesotrypsin. J Biol Chem 2008, 283:4115–4123 [PubMed: 18077447]
11. Salameh MA, Soares AS, Navaneetham D, Sinha D, Walsh PN, Radisky ES. Determinants of affinity and proteolytic stability in interactions of Kunitz family protease inhibitors with mesotrypsin. J Biol Chem 2010, 285:36884–36896 [PubMed: 20861008]
12. Salameh MA, Robinson JL, Navaneetham D, Sinha D, Madden BJ, Walsh PN, Radisky ES. The amyloid precursor protein/protease nexin 2 Kunitz inhibitor domain is a highly specific substrate of mesotrypsin. J Biol Chem 2010, 285:1939–1949 [PubMed: 19920152]
13. Pendlebury D, Wang R, Henin RD, Hockla A, Soares AS, Madden BJ, Kazanov MD, Radisky ES. Sequence and conformational specificity in substrate recognition: several human Kunitz protease inhibitor domains are specific substrates of mesotrypsin. J Biol Chem 2014, 289:32783–32797 [PubMed: 25301953]
14. Alloy AP, Kayode O, Wang R, Hockla A, Soares AS, Radisky ES. (2015) Mesotrypsin has evolved four unique residues to cleave trypsin inhibitors as substrates. J Biol Chem 2015, 290:21523–21535 [PubMed: 26175157]
15. Szilágyi L, Kénesi E, Katona G, Kaslik G, Juhász G, Gráf L. Comparative in vitro studies on native and recombinant human cationic trypsins. Cathepsin B is a possible pathological activator of trypsinogen in pancreatitis. J Biol Chem 2001, 276:24574–24580 [PubMed: 11312265]
16. Szepessy E, Sahin-Tóth M. Human mesotrypsin exhibits restricted S1’ subsite specificity with a strong preference for small polar side chains. FEBS J 2006, 273:2942–2954 [PubMed: 16759229]
17. Medveczky P, Antal J, Patthy A, Kékesi K, Juhász G, Szilágyi L, Gráf L. Myelin basic protein, an autoantigen in multiple sclerosis, is selectively processed by human trypsin 4. FEBS Lett 2006, 580:545–552 [PubMed: 16412431]
18. Wang Y, Luo W, Wartmann T, Halangk W, Sahin-Tóth M, Reiser G. Mesotrypsin, a brain trypsin, activates selectively proteinase-activated receptor-1, but not proteinase-activated receptor-2, in rat astrocytes. J Neurochem 2006, 99:759–769 [PubMed: 16903872]
19. Knecht W, Cottrell GS, Amadesi S, Mohlin J, Skåregärde A, Gedda K, Peterson A, Chapman K, Hollenberg MD, Vergnolle N, Bunnett NW. Trypsin IV or mesotrypsin and p23 cleave protease-

activated receptors 1 and 2 to induce inflammation and hyperalgesia. J Biol Chem 2007, 282:26089–26100 [PubMed: 17623652]

20. Sahin-Tóth M Human mesotrypsin defies natural trypsin inhibitors: from passive resistance to active destruction. Protein Pept Lett 2005, 12:457–464 [PubMed: 16029158]
21. Salameh MA, Radisky ES. Biochemical and structural insights into mesotrypsin: an unusual human trypsin. Int J Biochem Mol Biol 2013, 4:129–139 [PubMed: 24049668]
22. Geisz A, Sahin-Tóth M. A preclinical model of chronic pancreatitis driven by trypsinogen autoactivation. Nat Commun 2018, 9:5033 [PubMed: 30487519]
23. Jancsó Z, Sahin-Tóth M. Mutation that promotes activation of trypsinogen increases severity of secretagogue-induced pancreatitis in mice. Gastroenterology 2020, 158:1083–1094 [PubMed: 31751559]
24. Chen JM, Audrezet MP, Mercier B, Quere I, Ferec C. Exclusion of anionic trypsinogen and mesotrypsinogen involvement in hereditary pancreatitis without cationic trypsinogen gene mutations. Scand J Gastroenterol 1999, 34:831–832 [PubMed: 10499487]
25. Nemoda Z, Teich N, Hugenberg C, Sahin-Tóth M. Genetic and biochemical characterization of the E32del polymorphism in human mesotrypsinogen. Pancreatology 2005, 5:273–278 [PubMed: 15855826]
26. Masson E, Le Maréchal C, Chen JM, Férec C. Absence of mesotrypsinogen gene (PRSS3) copy number variations in patients with chronic pancreatitis. Pancreas 2008, 37:227–228 [PubMed: 18665091]
27. Rosendahl J, Teich N, Kovacs P, Szmola R, Blüher M, Gress TM, Hoffmeister A, Keim V, Löhr M, Mössner J, Nickel R, Ockenga J, Pfützer R, Schulz HU, Stumvoll M, Wittenburg H, Sahin-Tóth M, Witt H. Complete analysis of the human mesotrypsinogen gene (PRSS3) in patients with chronic pancreatitis. Pancreatology 2010, 10:243–249 [PubMed: 20484962]
28. Németh BC, Wartmann T, Halangk W, Sahin-Tóth M. Autoactivation of mouse trypsinogens is regulated by chymotrypsin C via cleavage of the autolysis loop. J Biol Chem 2013, 288:24049–24062 [PubMed: 23814066]
29. Király O, Guan L, Sahin-Tóth M. Expression of recombinant proteins with uniform N-termini. Methods Mol Biol 2011, 705:175–94 [PubMed: 21125386]
30. Lengyel Z, Pál G, Sahin-Tóth M. Affinity purification of recombinant trypsinogen using immobilized ecotin. Protein Expr Purif 1998, 12:291–294 [PubMed: 9518472]
31. Mosztbacher D, Jancsó Z, Sahin-Tóth M. Loss of chymotrypsin-like protease (CTRL) alters intrapancreatic protease activation but not pancreatitis severity in mice. Sci Rep 2020, 10:11731 [PubMed: 32678161]
32. Kereszturi E, Király O, Sahin-Tóth M. Minigene analysis of intronic variants in common SPINK1 haplotypes associated with chronic pancreatitis. Gut 2009, 58:545–549 [PubMed: 18978175]
33. Szabó A, Pilsak C, Bence M, Witt H, Sahin-Tóth M. Complex formation of human proelastases with procarboxypeptidases A1 and A2. J Biol Chem 2016, 291:17706–17716 [PubMed: 27358403]
34. Mosztbacher D, Demcsák A, Sahin-Tóth M. Measuring digestive protease activation in the mouse pancreas. Pancreatology 2020, 20:288–292 [PubMed: 31899136]
35. Wang J, Ohmuraya M, Suyama K, Hirota M, Ozaki N, Baba H, Nakagata N, Araki K, Yamamura K. Relationship of strain-dependent susceptibility to experimentally induced acute pancreatitis with regulation of Prss1 and Spink3 expression. Lab Invest 2010, 90:654–664 [PubMed: 20157294]
36. Dawra R, Sah RP, Dudeja V, et al. Intra-acinar trypsinogen activation mediates early stages of pancreatic injury but not inflammation in mice with acute pancreatitis. Gastroenterology 2011, 141:2210–2217 [PubMed: 21875495]
37. Sah RP, Dudeja V, Dawra RK, Saluja AK. Cerulein-induced chronic pancreatitis does not require intra-acinar activation of trypsinogen in mice. Gastroenterology 2013, 144:1076–1085 [PubMed: 23354015]
38. Singh VP, Bhagat L, Navina S, Sharif R, Dawra RK, Saluja AK. Protease-activated receptor-2 protects against pancreatitis by stimulating exocrine secretion. Gut 2007, 56:958–964 [PubMed: 17114298]

39. Hockla A, Radisky DC, Radisky ES. Mesotrypsin promotes malignant growth of breast cancer cells through shedding of CD109. Breast Cancer Res Treat 2010, 124:27–38 [PubMed: 20035377]

40. Jiang G, Cao F, Ren G, Gao D, Bhakta V, Zhang Y, Cao H, Dong Z, Zang W, Zhang S, Wong HH, Hiley C, Crnogorac-Jurcevic T, Lemoine NR, Wang Y. PRSS3 promotes tumour growth and metastasis of human pancreatic cancer. Gut 2010, 59:1535–1544 [PubMed: 20947888]

41. Hockla A, Miller E, Salameh MA, Copland JA, Radisky DC, Radisky ES. PRSS3/mesotrypsin is a therapeutic target for metastatic prostate cancer. Mol Cancer Res 2012, 10:1555–1566 [PubMed: 23258495]

42. Ma H, Hockla A, Mehner C, Coban M, Papo N, Radisky DC, Radisky ES. PRSS3/Mesotrypsin and kallikrein-related peptidase 5 are associated with poor prognosis and contribute to tumor cell invasion and growth in lung adenocarcinoma. Sci Rep 2019, 9:1844 [PubMed: 30755669]

43. Toldi V, Szabó A, Sahin-Tóth M. Inactivation of mesotrypsin by chymotrypsin C prevents trypsin inhibitor degradation. J Biol Chem 2020, 295:3447–3455 [PubMed: 32014997]

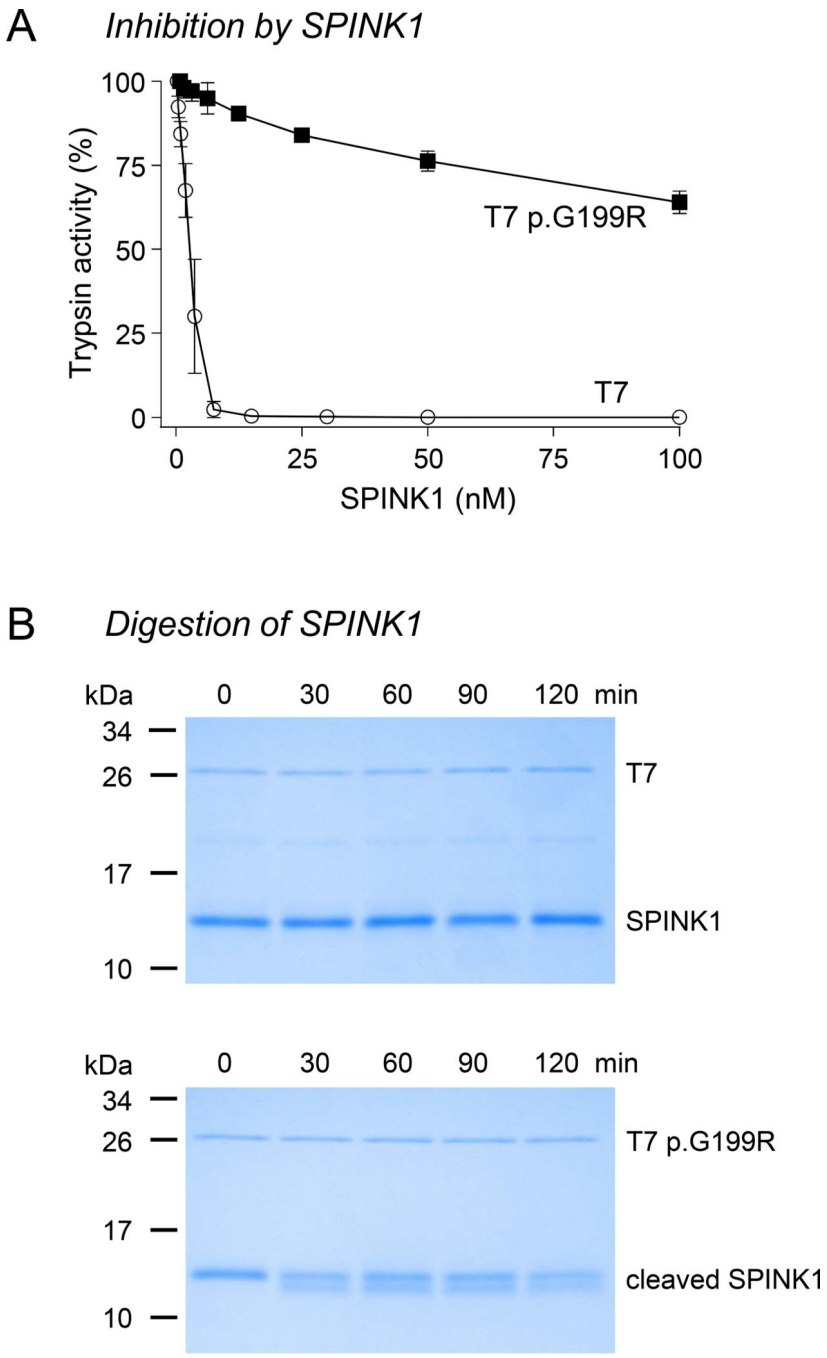

Figure 1.

Interaction of mouse SPINK1 with p.G199R mutant T7 trypsin. **A**, Inhibition of wild-type and p.G199R mutant T7 trypsin by mouse SPINK1. Data points represent the average of four measurements with SD indicated. **B**, Digestion of mouse SPINK1 by wild-type and p.G199R mutant T7 trypsin. N-terminal sequencing of the cleavage products indicated that the cleavage site corresponds to the Arg42-Ile43 reactive-site peptide bond. Representative gels from two experiments are shown. Experiments were performed as described in

Methods. Note that the calculated molecular weight of 10His-tagged mouse SPINK1 is 7.5 kDa, but it migrates anomalously, between the 10 and 17 kDa molecular weight markers.

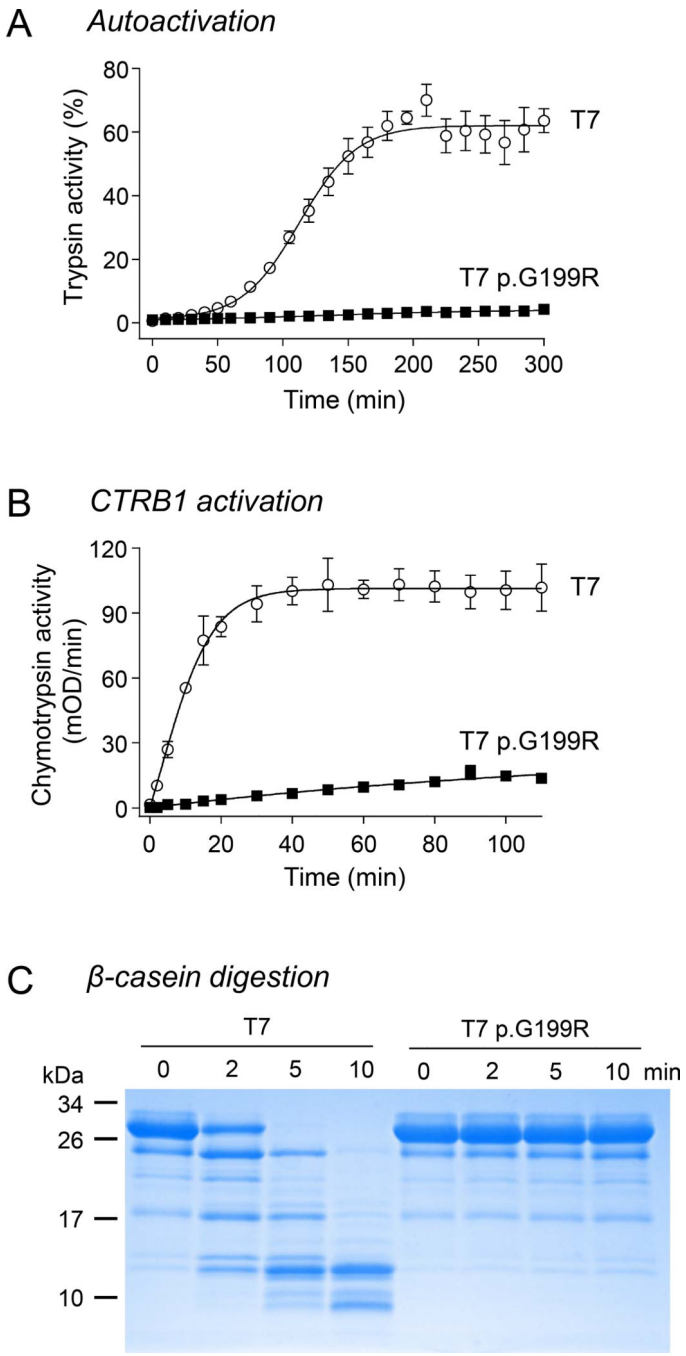

Figure 2.

Catalytic properties of p.G199R mutant T7 trypsin. **A**, Autoactivation of wild-type and p.G199R mutant T7 trypsinogen. **B**, Activation of mouse chymotrypsinogen B1 (CTRB1) by wild-type and p.G199R mutant T7 trypsin. Data points represent the average of two measurements with the SD indicated. **C**, Digestion of bovine ß-casein by wild-type and p.G199R mutant T7 trypsin. Representative gel from two experiments is shown. Experiments were performed as described in Methods.

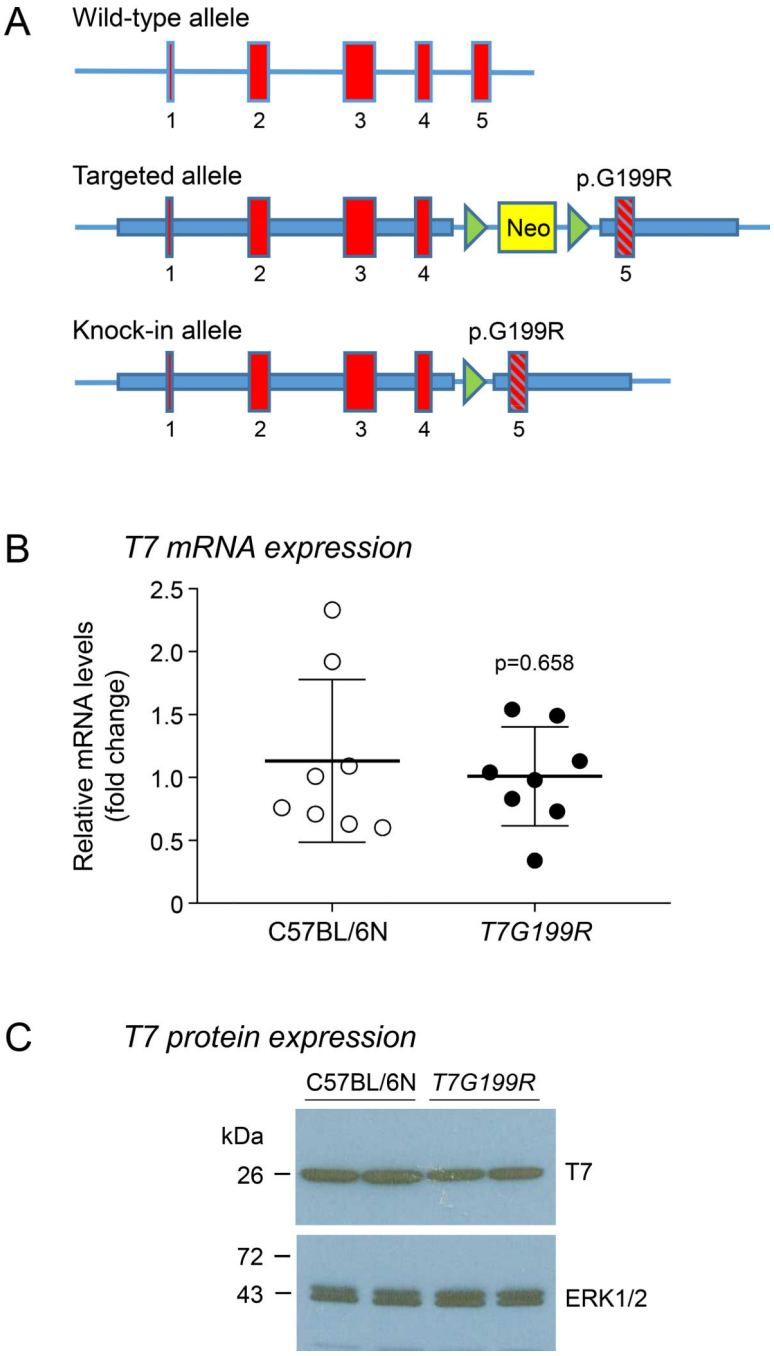

Figure 3.

Generation of the *T7G199R* mouse strain and expression of T7 trypsinogen. **A**, Schematic representation of the wild-type and recombined *T7G199R* alleles before and after excision of the neomycin cassette. See text for details. **B**, Expression of T7 trypsinogen mRNA in the pancreas of C57BL/6N and *T7G199R* mice. Quantitative reverse-transcription PCR was performed as described in Methods. Individual data points were graphed with the mean and SD indicated. The difference of means between two groups was analyzed by two-tailed unpaired t-test. **C**, T7 trypsinogen protein levels in the pancreas of C57BL/6N and *T7G199R*

mice. Western blotting was performed as described in Methods. Representative blot from two experiments is shown.

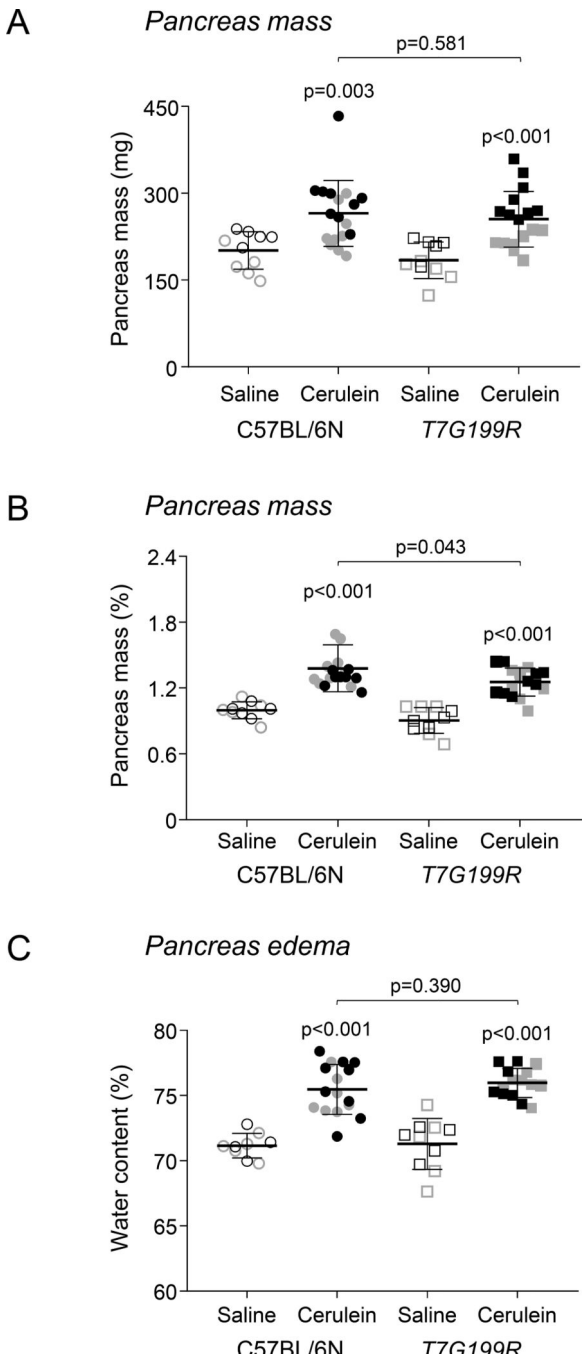

Figure 4.

Pancreas mass and pancreatic water content in cerulein-induced pancreatitis of *T7G199R* mice. C57BL/6N and *T7G199R* mice were given 10 hourly saline or cerulein injections, as indicated. Mice were sacrificed 1 hour after the last injection. **A**, Pancreas mass in mg units. **B**, Pancreas mass as percent of body mass. **C**, Pancreas water content expressed as percent of wet pancreas mass. Individual data points were graphed with the mean and SD indicated. Gray and black symbols denote female and male mice, respectively. The difference of means between two groups was analyzed by two-tailed unpaired t-test. See Methods for details.

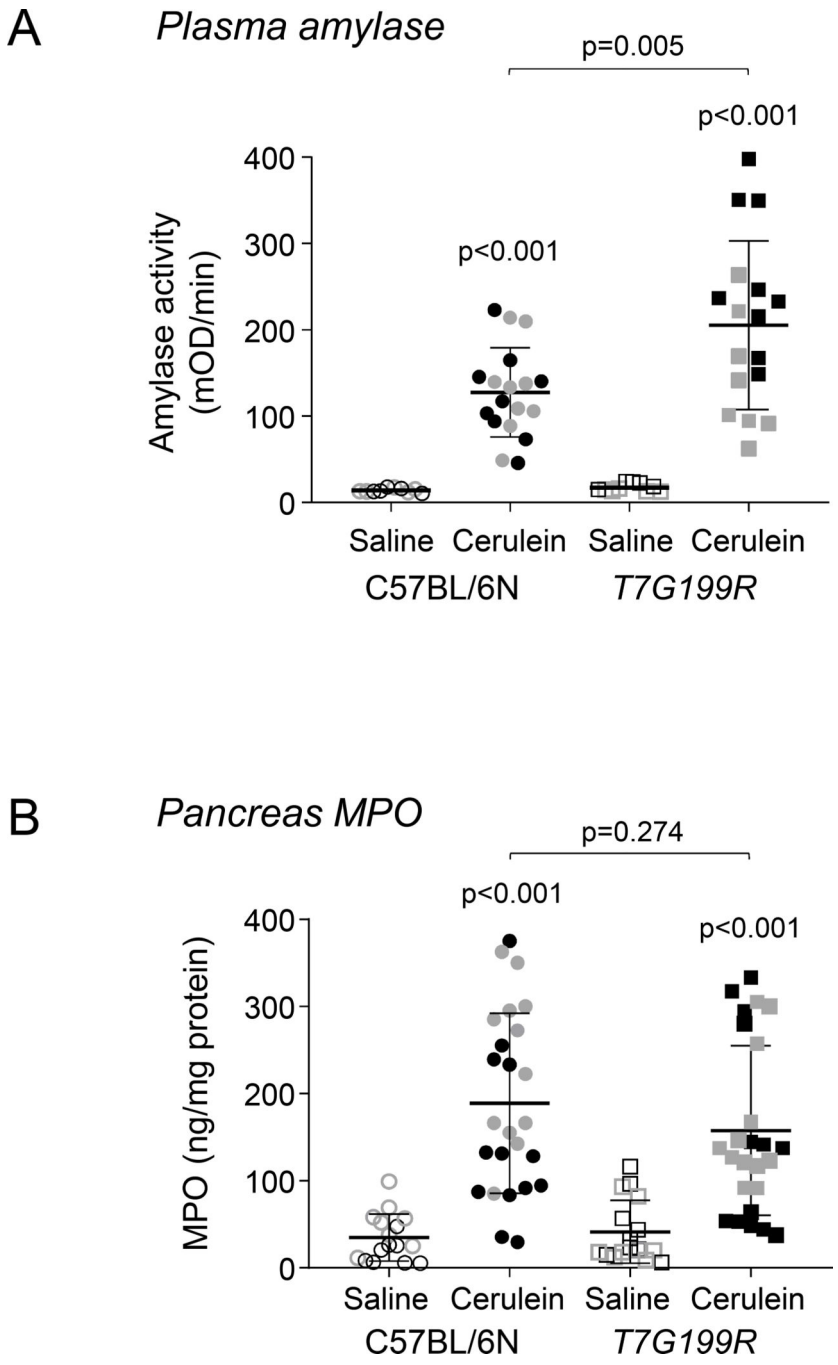

Figure 5.

Plasma amylase activity and pancreas myeloperoxidase (MPO) content in cerulean-induced pancreatitis of *T7G199R* mice. C57BL/6N and *T7G199R* mice were given 10 hourly saline or cerulein injections, as indicated. Mice were sacrificed 1 hour after the last injection. **A**, Plasma amylase activity. Note that a mOD/min substrate cleavage rate value corresponds to 23.8 U/L amylase activity. **B**, Pancreas MPO content. Individual data points were graphed with the mean and SD indicated. Gray and black symbols denote female and male mice,

respectively. The difference of means between two groups was analyzed by two-tailed unpaired t-test. See Methods for experimental details.

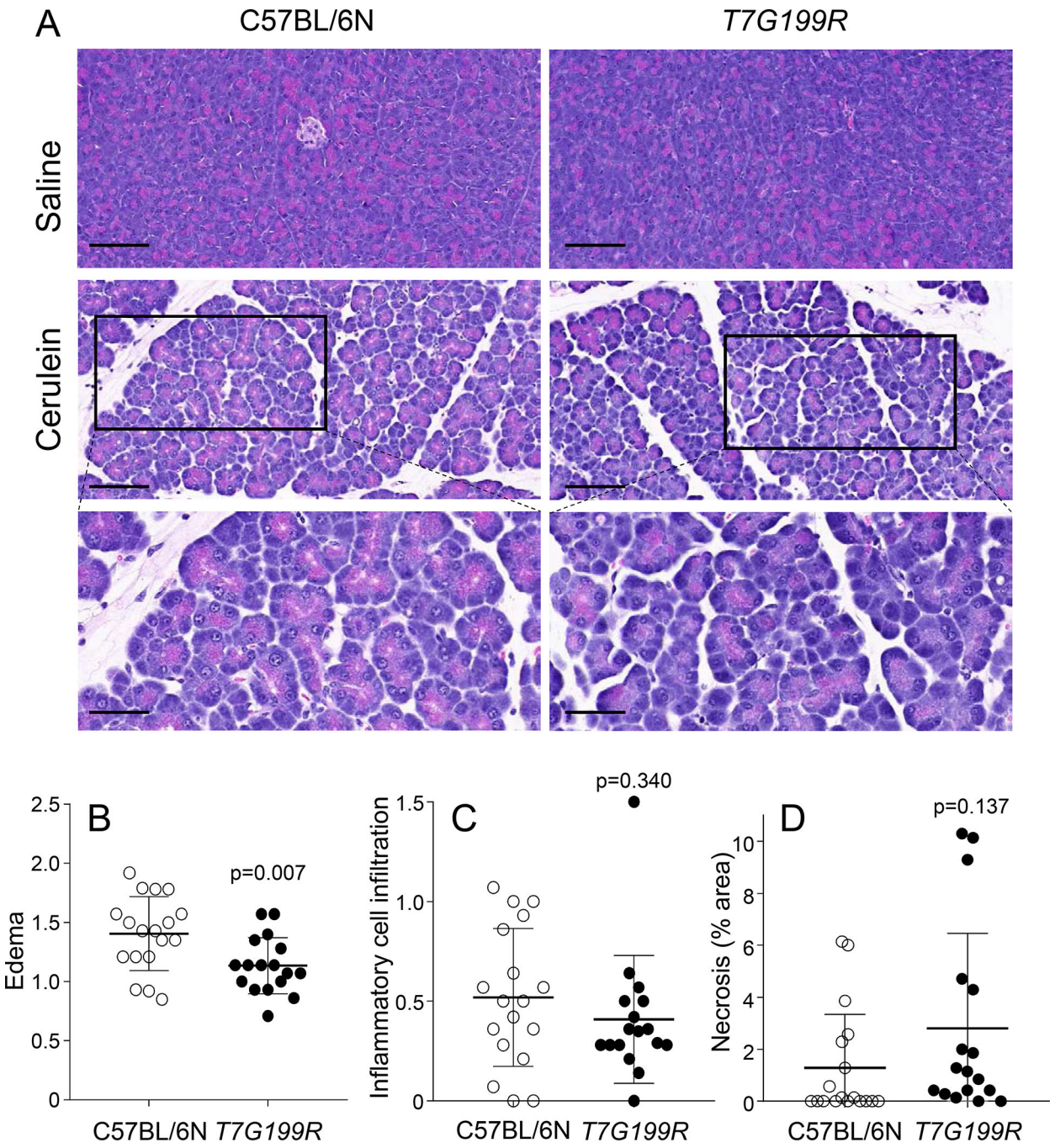

Figure 6.

Pancreas histology in cerulein-induced pancreatitis of *T7G199R* mice. C57BL/6N and *T7G199R* mice were given 10 hourly saline or cerulein injections, as indicated. Mice were sacrificed 1 hour after the last injection. **A,** Hematoxylin-eosin stained pancreas sections. The scale bars correspond to 100 μm (upper panels) and 50 μm (lower enlargements). Histology scoring of pancreas sections was performed for **B**, edema, **C,** inflammatory cell infiltration, and **D**, acinar cell necrosis. Individual data points were graphed with the mean

and SD indicated. The difference of means between two groups was analyzed by two-tailed unpaired t-test. See Methods for details.

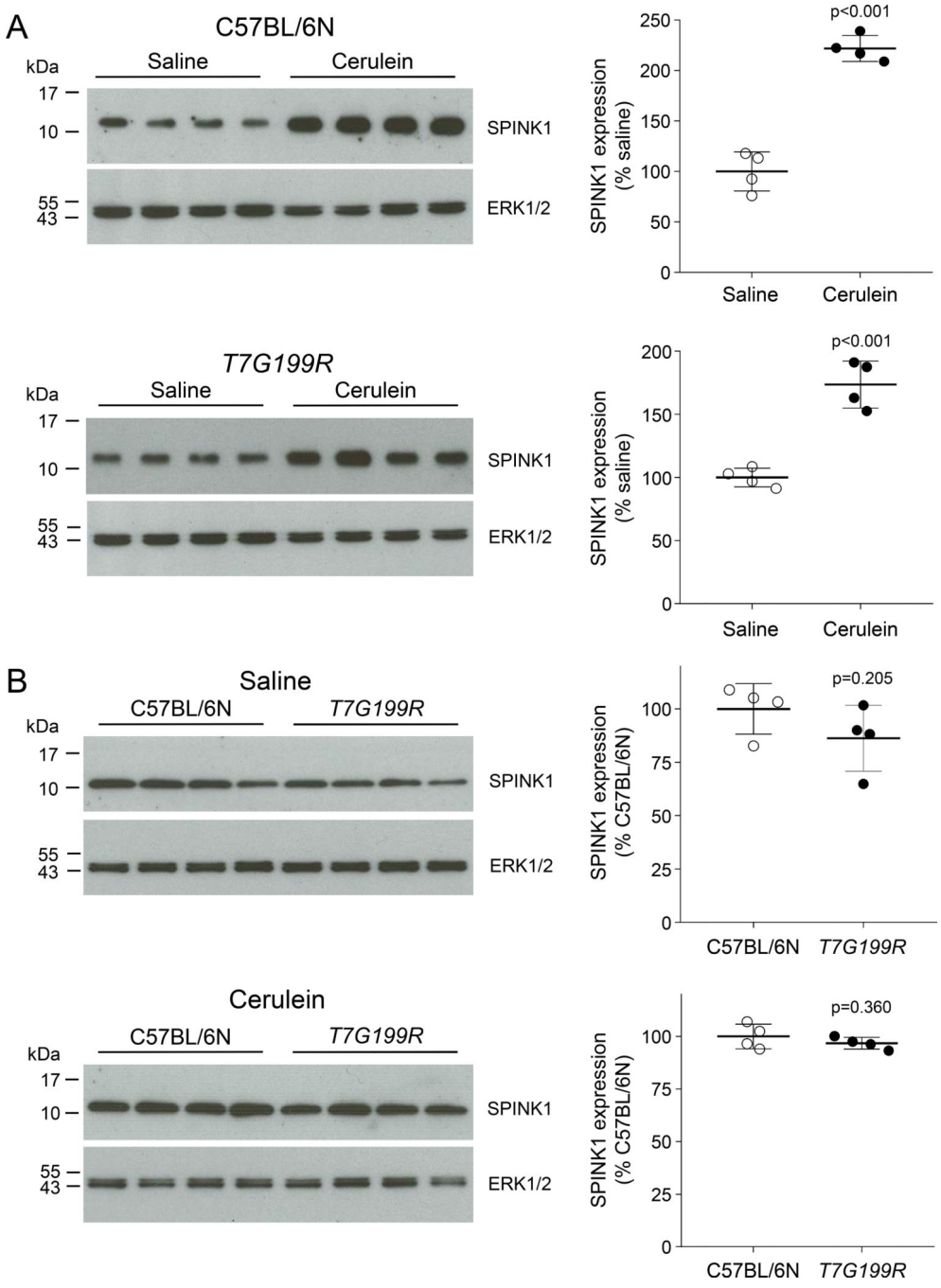

Figure 7.

SPINK1 expression in cerulein-induced pancreatitis of *T7G199R* mice. C57BL/6N and *T7G199R* mice were given 10 hourly saline or cerulein injections, as indicated. Mice were sacrificed 1 hour after the last injection and SPINK1 levels in pancreas homogenates were determined by western blotting. **A**, Upregulation of SPINK1 protein in cerulein-treated mice relative to saline-treated mice. **B**, Comparison of SPINK1 protein levels between C57BL/6N and *T7G199R* mice treated either with saline or cerulein. Graphs illustrate densitometric evaluations of the western blots. Individual data points were graphed with the mean and SD

indicated. The difference of means between two groups was analyzed by two-tailed unpaired t-test. See Methods for experimental details. Note that the 6.1 kDa mouse SPINK1 migrates anomalously, at or above the 10 kDa molecular weight marker.

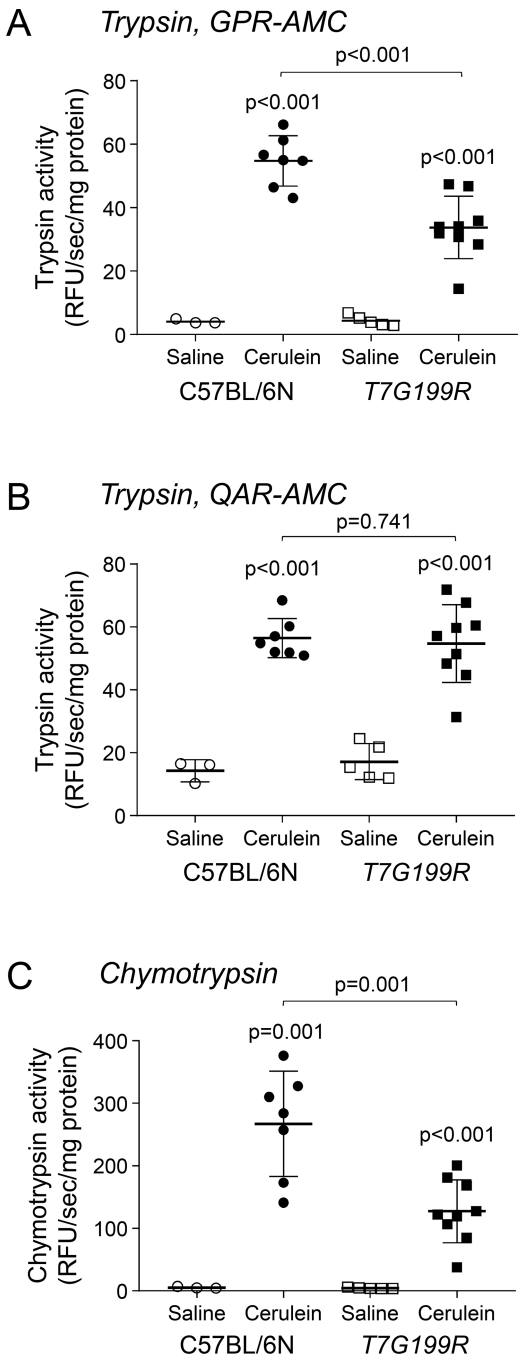

Figure 8.

Cerulein-induced intrapancreatic trypsin and chymotrypsin activation in *T7G199R* mice. C57BL/6N and *T7G199R* mice were given a single saline or cerulein injection, as indicated, and the mice were sacrificed 30 min later. **A**, Trypsin activity in pancreas homogenates measured with the Z-Gly-Pro-Arg-7-amino-4-methylcoumarin (GPR-AMC) substrate. **B**, Trypsin activity measured with the Boc-Gln-Ala-Arg-7-amino-4-methylcoumarin (QAR-AMC) substrate. **C**, Chymotrypsin activity in pancreas homogenates measured with the Suc-Ala-Ala-Pro-Phe-7-amino-4-methylcoumarin (AAPF-AMC) substrate. Individual data

points were graphed with the mean and SD indicated. The difference of means between two groups was analyzed by two-tailed unpaired t-test. See Methods for experimental details.

Table 1.

Kinetic parameters of wild-type T7 and p.G199R mutant trypsin on peptide substrates. Three experiments were fitted globally and the error of the fit is indicated. See Methods for details.

	k_{cat} (s^{-1})	K_M (μM)	k_{cat}/K_M ($M^{-1}·s^{-1}$)
Z-Gly-Pro-Arg-*p*-nitroanilide			
T7	73.7±1.3	29.9±1.6	2.5 x 10^6
T7 p.G199R	180.5±4.5	40.3±2.8	4.5 x 10^6
Z-Gly-Pro-Arg-7-amino-4-methylcoumarin			
T7	36.9±0.3	40.3±0.8	9.2 x 10^5
T7 p.G199R	18.6±0.1	97±1.2	1.9 x 10^5
Boc-Gln-Ala-Arg-7-amino-4-methylcoumarin			
T7	37.4±0.2	8.2±0.2	4.6 x 10^6
T7 p.G199R	66.8±2.2	70.4±5.3	9.5 x 10^5